Assessment of ductile dike behavior as a novel flood risk reduction measure

den Heijer, F.; Kok, M.

DOI
10.1111/risa.14071

Publication date
2022

Document Version
Final published version

Published in
Risk Analysis

Citation (APA)
den Heijer, F., & Kok, M. (2022). Assessment of ductile dike behavior as a novel flood risk reduction measure. *Risk Analysis*, *43*(9), 1779-1794. https://doi.org/10.1111/risa.14071

DOI: 10.1111/risa.14071

ORIGINAL ARTICLE

Assessment of ductile dike behavior as a novel flood risk reduction measure

F. den Heijer[1] | **M. Kok**[2]

[1]Department of Sustainable River Management, HAN University of Applied Sciences, Arnhem, The Netherlands

[2]Department of Hydraulic Engineering, Faculty of Civil Engineering and Geosciences, Delft University of Technology, Delft, The Netherlands

Correspondence
F. den Heijer, Department of Sustainable River Management, HAN University of Applied Sciences, Ruitenberglaan 26, 6826 CC Arnhem, The Netherlands.
Email: frank.denheijer@han.nl

Abstract

Dikes are an effective flood risk reduction measure in deltaic areas. Present risk analyses consist often of decoupled calculations of probabilities of dike failure and calculation of consequences of flooding given dike failure. However, the flood defense design determines not only the probability of failure, but influences the consequences of flooding as well. Especially when the dike has a ductile failure and breach growth behavior, due to a structural robust design, the consequences of flooding reduce. In this article, we present a novel assessment of risks and investments, valuing structural robustness of a construction type, represented by its ductile behavior during high loads. Therefore, the consecutive occurrence of initial dike failure mechanisms, failure path development, breach growth, and consequences is modeled integral and time-dependent. The investments consist of the costs to reinforce or reconstruct the flood defense to behave relatively ductile. This integral assessment enables to compare flood impacts of different construction types and different dimensions of designs. We applied it on a case in a riverine area in the Netherlands. The results show that the total societal costs and the individual risks on victims are very dependent on the construction type. The risk profile of a polder protected by a brittle or a ductile dike differs significantly. The brittle sand dike in the case requires larger dimensions than the more ductile dike with a clay core.

KEYWORDS
dike construction type, flood risk, optimalization, probabilistic

200-CHARACTER SUMMARY

We present a new approach for optimal investment in dike reinforcement, in which extra flood risk reduction is taken into account due to valuing ductile dike behavior, illustrated by a case study.

1 | INTRODUCTION

Dikes are crucial for flood risk management in the lower reach of rivers (van de Ven, 2004). Aging, climate change, and human and faunal activities urge to maintain and reinforce or adapt them. Increase of data, knowledge, and innovations provide the opportunity to manage these activities in a contemporary manner. Risk is mostly defined as probability of flooding times consequences (Jonkman et al., 2016). In hydraulic engineering, flood risk is a concept that concerns both the possible impact of flooding and the probability that it will occur (Kok et al., 2017). In fact, mainly three categories of flood risk reduction measures are practiced: reduction of loads, increase of strength, both reducing the probability of failure, or reduction of consequences of dike failure. In this article, we present a fourth one: structural robustness by design of the dike construction.

Baker et al. (2008) introduced a framework for assessing robustness. Klerk (2022) investigated structural robustness of dike revetments. In this article, we elaborate structural

robustness of the dike related to flood risks. Structural robustness can be increased by a ductile behavior of the construction. We define ductile behavior as the slow failure process of a dike, and a relatively slow or depth-limited breach growth, both leading to reduced breach dimensions and reducing flood impacts. It is the opposite of brittle behavior, with a sudden occurrence of a breach, increasing flood impacts. Thus, a more ductile dike is not necessarily larger than a brittle dike but has another construction with, for example, a clay core instead of a sand core, leading to less flood impact. We developed a method to evaluate the potential benefits, and we applied it on a location in the Dutch river area.

In the Netherlands, flood risk reduction has always been important. About 60% of the Netherlands is flood prone (Kok et al., 2017). Dikes have been built from the early middle ages. In former days, the height and construction of dikes were mainly based on experience. After the disaster in 1953, during which 1836 people died (Slager, 2003), a more scientific and statistical-quantitative approach was developed for the practice of flood defense management. Safety standards were established based on simplified risk assessments (van Dantzig, 1956), resulting in water levels to be safely withstood by the dikes. Design rules were developed, dikes were strengthened, and storm surge barriers have been built (van de Ven, 2004). Since 1996, a periodic assessment is required, executed every 12 years at present, to compare the actual dike condition of each individual dike section with the standards. In practice, the dike cross sections that are considered to be most representative are used to assess these dike sections.

This article's first motive is to enable an evaluation and enrichment of the grown practice. In Sayers et al. (2002), the source-pathway-receptor framework figures out a route to an effective flood risk management. However, we observe a practice to design mainly to meet the standards with minimal financial efforts, leading to a preference of brittle dikes with a sand core. This may have worked out this way due to the standards and rules for safety assessment as provided in Slomp et al. (2016), or due to financial constraints. The approach used in the development of the standards, to propose more stringent standards at high-risk locations, leads to stronger but still brittle dikes. We barely found research on whether this is an optimal choice (Bischiniotis et al., 2018; den Heijer, 2021). However, the practice before standards were established was to build dikes, especially on high-risk locations, with a core of clay (Halter et al., 2018), such as the Grebbedijk. The DeltaCommision (2008) introduced the so-called Delta dikes, which are so high, strong, and wide that dike failure probability is very small with respect to other dikes. The elaborations of Delta dikes are a step to search for alternative construction types for high-risk locations (de Bruijn & Klijn, 2011; Knoeff & Ellen, 2012), and field tests with a sheetpile in the dike, at Eemdijk, showed the tough failure behavior (Breedeveld et al., 2019). This research responds to the growing awareness of the importance of dike construction at high-risk locations, with an approach providing comparative insights in its societal benefits.

Second motive for this article is to provide an extra opportunity for the utilization of the recently updated safety standards. The standards are based on an improved and extended risk analysis (Kind, 2014; Ministerie van Infrastructuur en Milieu, 2016), expressed as acceptable flooding probabilities of dike segments. The segments consist of a series of dike sections. Only the failure mechanisms overtopping and piping are considered, assuming that these would be normative for the dike dimensions. Expecting these simplification and generalization of risk-based standards could not be optimal for some of the situations, the policy provides the so-called decision for "exchange" between measures for reduction of failure probability and reduction of consequences, persevering the same risk level (Kok et al., 2017). This provides the opportunity to incorporate differences in consequences of failure as well, due to different failure behavior in time, dependent on initial failure mechanism or construction type. The fourth category of risk reduction measures, referred to in the preamble of this paragraph, may provide an opportunity to take benefit of this "exchange" policy, reflected in adapted dimensions, adapted construction type or adapted optimal flood risk level.

Third motive is to enrich the present elaboration of time-dependent failure processes in the reliability analyses of dikes (Kortenhaus & Oumeraci, 2009; te Nijenhuis et al., 2020; Rosenbrand & Knoeff, 2020; van Hoven, 2014; van den Ham, 2020), describing the residual strength after occurrence of an initial failure mechanism. The present methods for system analysis, developed in the decades of preparation of the new standards, do not support time-dependent failure approaches. Loads are schematized by extreme value statistics of maximal water levels during storm or river floods. In essence, the present analysis is compiled by a combination of a probabilistic analysis per failure mechanism per dike section, and a system analysis of all known failure mechanisms and dike sections in a flood defense segment (Steenbergen & Vrouwenvelder, 1999; Steenbergen et al., 2004; van Westen, 2005; VNK2, 2011). To embed time-dependent developments of initial failure mechanisms and time-dependent failure paths to flooding require artificial assumptions, such as the average duration of a water level or storm maximum (van den Ham, 2020). This article provides a method setup to handle time dependency, avoiding the uncertainties connected to these artificial assumptions.

The objective of this article is to develop and apply a method that will enable the evaluation of the risk reduction potential of dike construction types. We consecutively present the theoretical background of flood risk assessment, risk-based criteria as a basis for trade-offs, the methodology and application of the proposed evaluation of ductile behavior, a case study, and finally the discussion and conclusions.

2 | THEORETICAL BACKGROUND

2.1 | Flood risk

Risk is mostly defined as a function of the probability P of an undesired event i and its consequences d (Jonkman et al., 2016; Kaplan and Garrick, 1981; Kok et al., 2017). In this article, we define risk as probability times consequences. The expected value $E(d)$ is the sum of the risk for all possible scenarios leading to that undesired event (Jonkman et al., 2016):

$$E(d) = \sum_{i=1}^{i=n} P_i \cdot d_i \tag{1}$$

In fact, the number of flooding scenarios is infinite. Kaplan and Garrick (1981) already proposed to take into account the whole risk curve, and the uncertainties in these curves. Nevertheless, they understand the need to get a single value for the risk. Therefore, they already proposed to use utility functions to trade-off different types of consequences to reflect risk aversion. Using the expected value in (1) reflects a risk-neutral approach that is usual for economic optimizations in flood risk management (Eijgenraam, 2006; Kind, 2014).

For flood risk in low lying areas protected by dikes, the undesired event is flooding, most likely due to dike breach due to natural hazards anywhere along a dike segment (Kok et al., 2017; Sayers et al., 2002). The probability of flooding is expressed as the probability per year P_f of dike breach. The consequences of flooding are expressed as economic damage and victims (Kok et al., 2017).

In the application in the Netherlands, due to a smart choice of the dike segments, the consequences of dike breach are almost independent of the location of dike breach along a dike segment. Only a few scenarios expressing the effect of different load levels on the consequences are chosen: some individual breaches and one with multiple breaches as a worst case. This simplifies the risk calculation in de Bruijn and van der Doef (2011), distinguishing the calculations of dike failure and consequences:

$$E(d) = P_f \sum_{i=1}^{i=n} \alpha_i \cdot d_i \tag{2}$$

in which α_i is a weighting factor dependent on the chosen flooding scenarios i. A typical time pattern of the water level in the polder is given in Figure 1(A). The consequences are in de Bruijn and van der Doef (2011) related to the maximum water level and the maximum rate of water level increase during a flood. In this way, the calculations for dike failure are disconnected from the calculations of consequences. This simplified risk calculation contains predefined loads in time, the moment of dike failure, and breach growth in time. Since these are chosen independent of dike construction type, risk calculation in de Bruijn and van der Doef (2011) will not provide insight in the effects of construction type on the risks.

Therefore, in this study, we stick to the definition of risk in Equation (1), applying it for flood risk in such a way insight in the effects of construction type could be provided. We define the undesired event i as the occurrence of a flood at a location a (Figure 1B), resulting in a certain water level in time $h(t)$ during the flooding at that location (Figure 1C). The consequences d are defined as damage and victims during the event at a location a in a polder with surface and bathymetry A_b. The flood patterns $h(t)$ at a contain the characteristics of the loads on the dike system $S(t)$, the strength and construction of the dike R, the breaching behavior $B(t)$, and the bathymetry of the polder A_b:

$$h_{\vec{X},a}(t) = f(S(t), R, B(t), A_b) \tag{3}$$

with $\vec{X}$ the set of variables determining loads, strength and breach growth. In the Appendix, these variables and the physical relationships for determination of $h_{\vec{X},a}(t)$ are given as used for this study. The derivation of the probability of occurrence of a flood on a location in a polder is similar to the derivation of the probability of failure of a dike, based on loads and strength. The difference is the introduction of a chain of relationships following initial failure mechanisms, covering the whole pathway from "source" (hazard) to "receptor" (consequences) (Sayers et al., 2002). The probability of a flood pattern $h_{\vec{X},a}(t)$ depends on the set of uncertain variables $\vec{X}$ in the relations in Equation (3). In general, Equation (1) for the flood risk in a polder then looks like:

$$E(d) = \int_{a \in A_b} \int_{\vec{X}} \left(f_{\vec{X}}(h_{\vec{X},a}(t)) \cdot d(h_{\vec{X},a}(t)) \right) d\vec{X}\, da \tag{4}$$

in which $f_{\vec{X}}(h_{\vec{X},a}(t))$ is the probability density of the flooding at a with the flooding characteristics $h_{\vec{X},a}(t)$. Note the probability of failure of the dike is no longer a separate and disconnected part of this relation, but integrated in the derivation of the probability density function. Consequently, the probability density in Equation (4) contains the characteristics of the loads on the dike system, the strength and construction of the dike, and the characteristics of the polder.

A typical profile of the relation between river hazards and flood impact due to dike breach is given in Figure 2. The profile is based on the simplification to assume only maximum water level during a flood event as a cause for dike breach. River flood waves with relatively low maxima do not lead to any flood impact. When the maximum water level during a river flood wave exceeds a certain level, the dike breaches and the polder will be flooded, resulting in a sudden increase of maximum water level in the polder. This will only slightly increase with increasing maximum river water level (Figure 2A), see also Mens (2015). The frequency of exceedance decreases for higher river water levels (Figure 2B). The consequences correspond with the polder water level, occurring suddenly at a certain exceedance frequency and increasing slightly with decreasing exceedance

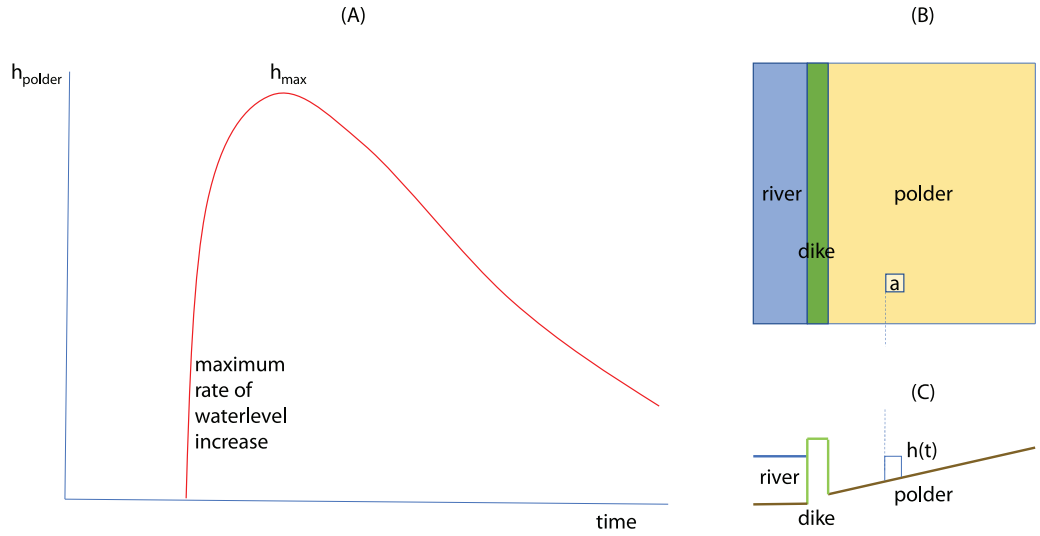

FIGURE 1 Typical pattern of the water level in the polder in time during a flood (A) in a polder in a riverine area (B) at location *a* (C).

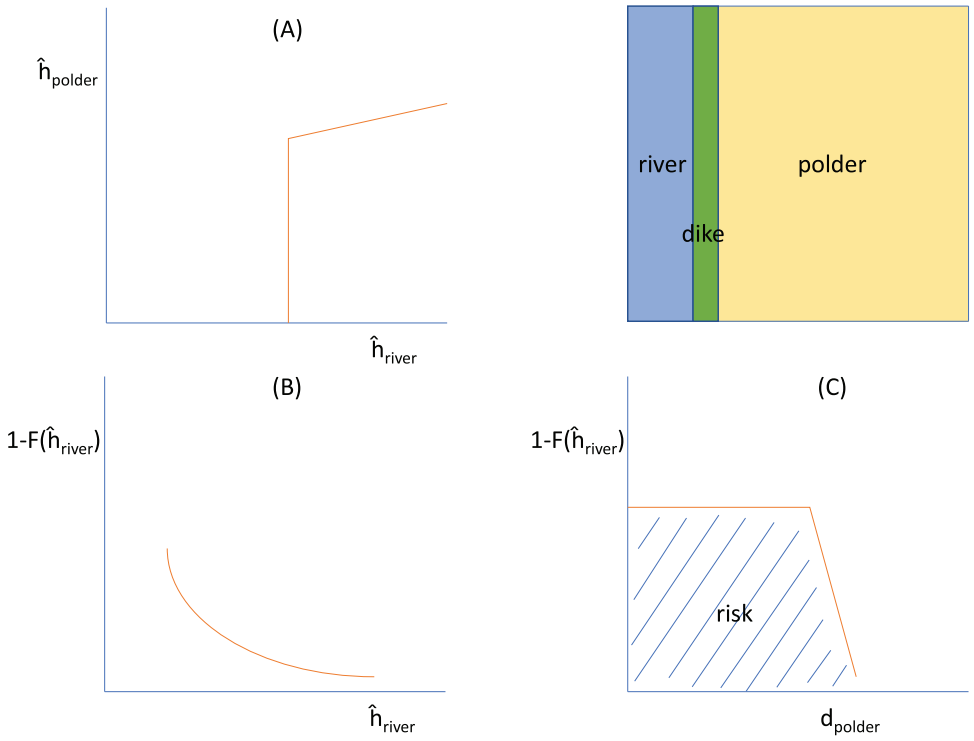

FIGURE 2 Typical relations in an riverine area protected by dikes between (A) maximum polder water level and maximum river water level; (B) maximum river water level and its exceedance frequency ($1 - F(\hat{h}_{river})$); and (C) damage in the polder and exceedance frequency of water level in the river. The surface below the curve in (C) is the risk assessed by Equation (4).

frequency (Figure 2C). Note that when the exceedance frequency of maximum water level in the river is directly related to the probability of dike breach, the surface below the profile of Figure 2(C) is the risk of flooding, corresponding to Equations (1) and (4). Note that the consequences d are multidimensional, mostly economic damage and victims. The shape of Figure 2(C) is referenced to as F_N-curve for groups of victims and F_D-curve for economical damage.

2.2 | Risk-based decision framework

To evaluate whether measures to reduce flood risks are beneficial the actual risk of flooding in Equation (4) with risk criteria. The safety standards in the Netherlands are expressed as probabilities of flooding of a dike segment. These are based on a risk-framework consisting of criteria for the individual, societal, and economical risks (Vrijling et al., 1995, 1998).

Since the societal risks are not generally used in decision frameworks, we took only the individual and economical risks. For the individual risk, the consequences d_{nv} in Equation (4) are expressed in the expected number of victims per year. For the ER, d_{ER} is expressed in the expected damage in €, per year.

The criterion on individual risk limits the probability of occurrence of an individual victim being on a location (local individual risk [LIR]):

$$E(d_{nv}) < LIR_{\max} \tag{5}$$

with d_{nv} the number of victims and $E(d_{nv})$ the expected value of the probability per year of a victim, being on a location, anywhere in the polder behind the dike segment of interest. In the Netherlands, the LIR is defined as the postal code averaged maximum in the polder protected by this dike segment, with $LIR_{\max}$ equal to 10^{-5} per year. Note that d_{nv} depends on the mortality given a flooding, which depends on the characteristics of flooding $h_{\vec{X},a}(t)$ in Equation (3). Substituting the general approach in Equation (4) for the limit on individual risks on location a gives:

$$\forall a : E_a(d_{nv}) = \int_{\vec{X}} \left(f_{\vec{X}}(h_{\vec{X},a}(t)) \cdot d_{nv}(h_{\vec{X},a}(t)) \right) d\vec{X} < LIR_{\max} \tag{6}$$

The criterion on ER is no limit but an optimization of the societal costs SC, the sum of costs of risk reduction measures and the net present value (NPV) of remaining economic risks (ERs). In, for example, Kind (2014) and Jonkman et al. (2016), the decision parameter in this optimization is the probability of failure of a dike, P_f. However, in the approach used in this article, the decision parameters are the dimensions and construction type of the dike, denoted as $\vec{Y}$ with $\vec{Y} \cup \vec{X}$. The probability of failure of a dike is only a side result of risk calculations with these parameters. The ER is defined as the sum of economic damage and the values of human lives lost in the polder (Kind, 2014):

$$E_{A_b}(d_{ER}) = E(d_D) + \int_{a \in A_b} E_a(d_{nv}) \cdot VOHL \, da \tag{7}$$

with $E_{A_b}(d_{ER})$ the ERs due to flooding in the polder behind the dike system of interest, and VOHL the (political determined) economic value of a human life. $E(d_D)$ can be defined substituting the general approach of Equation (4):

$$E(d_D) = \int_{a \in A_b} \int_{\vec{X}} \left(f_{\vec{X}}(h_{\vec{X},a}(t)) \cdot d_D(h_{\vec{X},a}(t)) \right) d\vec{X} \, da \tag{8}$$

with $d_D(h_{\vec{X},a}(t))$ the economic consequences of flooding on location a in the polder, with characteristics of flooding $h_{\vec{X},a}(t)$. The criterion on ERs is found by minimization of investments I for risk reduction measures and present value of remaining risk:

$$SC_{opt} = MIN_{\vec{Y}} \left(I + \frac{E_{A_b}(d_{ER})}{r} \right) \tag{9}$$

In which r is the interest rate and SC_{opt} the optimal present value of societal costs.

3 | APPLICATION

3.1 | Calculation of maximum polder water level due to flooding

Loads, strength, breach, flooding, and consequences are to be calculated time-dependent during a load event, for each of which numerical models could be used. Especially the calculation of Equation (3) is time-consuming. To be able to apply it for a proof of concept in a concrete riverine situation, simplifications have been made on the following physical relations and modeling:

- Loads during breach: The effect of the breach on the local water level is analytically derived, based on a polynomic relationship between discharge and water level, and the logic that the sum of discharges through the breach and in the river downstream should be equal to the upstream river discharge. See the Appendix for the physical relations.
- Dike system: The dike segment consists of exactly one dike section. Only two relevant initial failure mechanisms are considered, which are overtopping and piping. The piping mechanism is a regressive tunnel erosion process. The point at the riverside of the dike where the pipe shortcuts with the water system is called the entrance point, the point at the polder side the exit point. Two possible exit points are considered: the inner toe of the berm and the inner toe of the inner slope.
- Breaching: The dike failure path due to overtopping as an initial failure mechanism occurs when consecutively the inner revetment is eroded, the clay layer below the revetment is eroded, and the core is eroded. The dike failure path due to piping as an initial failure mechanism occurs when a pipe propagates entirely from exit backward to entrance point. See the Appendix for the physical relations.
- Flooding: The flooding in the polder area is schematized as a 0-D hydraulic model and the polder is flat. Thus, each inflow is directly spread over the polder with surface A, translating $h_{\vec{X},a}(t)$ into $h_{\vec{X}}(t)$.
- Consequences: The consequences of flooding are directly related to the flood inflow V, the total volume of water that entered the polder during the event. The relation is based on the National Database of Flood Simulations in Helpdesk Water (2020). The Appendix shows that this is a rather accurate simplification, especially for flood volumes larger than ca. 0.5×10^9 m^3.

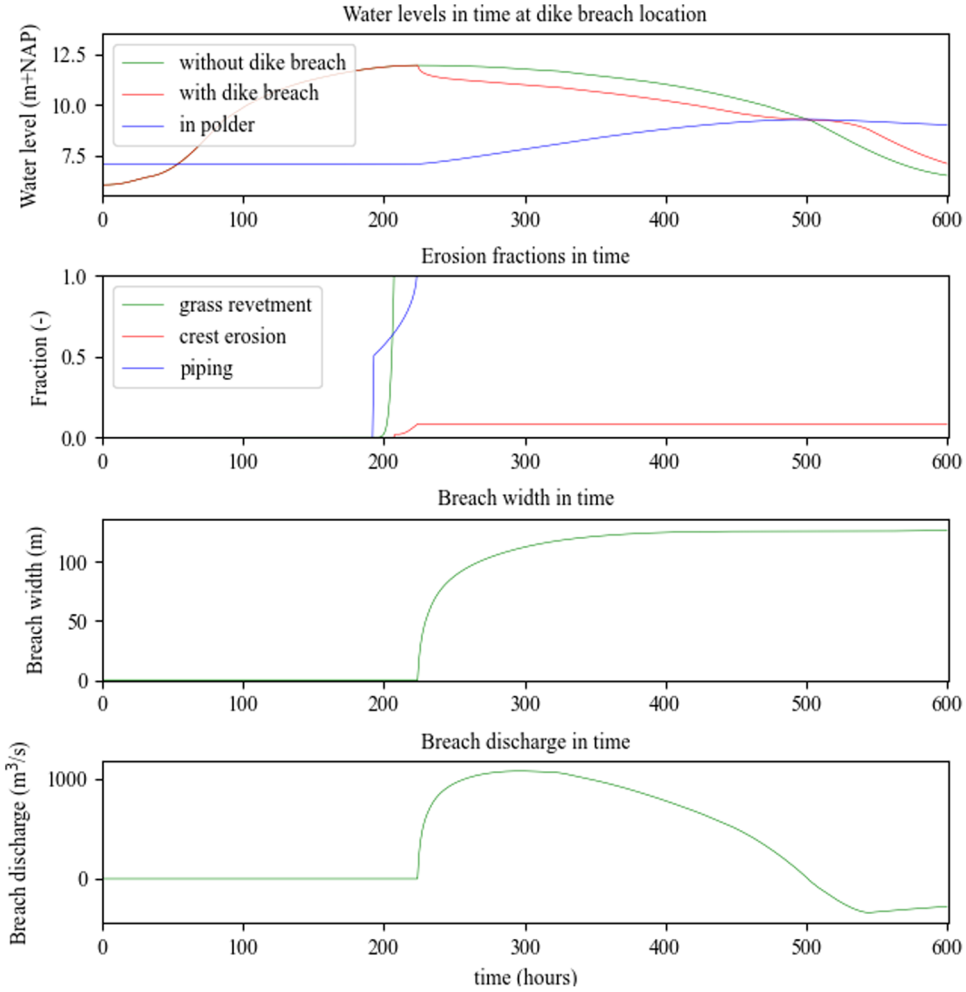

FIGURE 3 Example of calculation of, respectively, water levels in the river and in the polder as a part of the limit state function, erosion fractions in time, breach width in time, and breach discharge in time, for a location at Rhine river km 906.3, and a dike with a clay core with sheetpile.

The simplifications mean that the consequences of a flooding are only related to the maximum water level in the polder. The consequences of a flooding with a water level in the polder H are modeled as:

$$d = c_d \cdot V = c \cdot A \cdot H \tag{10}$$

with $c_d = 18.6$ Euro/m^3 for ERs d_{ER} and $c_d = 1.2 \times 10^{-6}$ victims/m^3 for the individual risk d_{nv}. The effect of time-dependent breach behavior, the core of this article, is processed in the calculation of the simplified equation (3), and thus, is still a part of the output since:

$$\widehat{h}_{\vec{X}} = MAX(h_{\vec{X}}(t)) \tag{11}$$

The time-dependent development during a flood event is modeled by a chain of physical relations, operationalized in a Python script and tested for a location along the Rhine river. The script for each of the physical relationships explained in the Appendix is checked separately before use in the model chain. In Figure 3, a set of intermediate results is showed of the propagation of the event in time in the physical space. The figure on top shows the development of the local water levels in time. The green line presents the undisturbed river water level in case of no breach. The river water level (red line) shows a jump when dike breach occurs at about $t = 220$ h. The polder water level (blue line) increases after dike breach and decreases when it exceeds the river water level. The second figure shows the erosion of the dike due to increasing loads. It shows the prelude of dike breach. At about 190 h, the piping mechanism starts with uncontrolled pipe growth (blue line). The pipe at that moment has grown to half the available length (fraction 50%). The green line shows the erosion of the grass cover on the inner slope due to overtopping. A fraction of 100% means that the cover is at least at one location damaged in a way the underlying core material cannot be protected anymore. Erosion of the core starts after such an eroded cover (red line). The two failure paths piping and overtopping develop simultaneously. In this case, dike breach is initiated by piping. The third figure shows the development of breach width. The last figure shows the inflow in the polder during the event. The integral of the inflow during the event, in this case between $t = 220$ h until $t = 500$ h, is the volume

V that can be used to calculate the consequences conform equation (10).

3.2 | Calculation of risks

Substituting these simplifications in Equation (4) leads to:

$$E(d) = A \cdot \int_{\vec{X}} \left(f_{\vec{X}}(\hat{h}_{\vec{X}}) \cdot d(\hat{h}_{\vec{X}}) \right) d\vec{X} \tag{12}$$

Substituting Equation (10) for a given level H gives the risk due to floodings causing a polder water level of H:

$$E(d \mid \hat{h}_{\vec{X}} = H) = A \cdot \int_{\vec{X}} \left(f_{\vec{X}}(H) \cdot c_d \cdot H \right) d\vec{X} \tag{13}$$

with $f_{\vec{X}}(H)$ the probability density of occurrence of H. Reordering Equation (13) and integration over all possible polder water levels H gives:

$$E(d) = A \cdot c_d \cdot \int_H H \cdot \int_{\vec{X}} \left(f_{\vec{X}}(H) \right) d\vec{X}\, dH \tag{14}$$

The part behind the second integral of Equation (14) is the probability of exceedance of polder water level H.

3.3 | Calculation of flood-level exceedance probabilities

The limit state function for exceedance of level H is:

$$Z(H) = H - \hat{h}_{\vec{X}} \tag{15}$$

where $P(Z < 0)$ follows the probability of exceedance of polder water level H : $P(\hat{h}_{\vec{X}} > H)$. For application in Equation (14), this probability has to be calculated for all H, which in practice means the domain $0 < H <$ dike crest:

$$\forall H \in (0, \textit{dike crest}) : P(\hat{h}_{\vec{X}} > H) = \int_{\vec{X}} \left(f_{\vec{X}}(H) \right) d\vec{X} \tag{16}$$

An example of the result of calculation of Equation (16) is showed in Figure 4. In this example, a series of calculations has been carried out for discrete values of H starting with $H_{\min} = 0.1$ m and a step $\triangle H = 0.2$ m. Note the relationship with existing approaches using the probability of failure of the dike P_f. This is a specific case of Equation (16) with $H \downarrow 0$, the intersection of the curve with the vertical axis:

$$P_f \approx \lim_{H \downarrow 0} P(\hat{h}_{\vec{X}} > H) \tag{17}$$

For H smaller than $H_{\min}$, we assume $= P(\hat{h}_{\vec{X}} > H) = P(\hat{h}_{\vec{X}} > H_{\min})$. With the result of this calculations, the risk in Equation (14) can be calculated easily by numerical integration:

$$E(d) = A \cdot c(d) \cdot \left(H_{\min} \cdot P(\hat{h}_{\vec{X}} > H_{\min}) + n \triangle H \cdot \sum_{i=1}^{i=n} P(\hat{h}_{\vec{X}} > \overline{H}) \right) \tag{18}$$

with $n = \frac{H_{dike\ crest}}{\triangle H}$, d and $c(d)$ indicating the type of risk, $P(\hat{h}_{\vec{X}} > \overline{H})$ the mean probability in the interval $(H - \triangle H, H)$ of polder water level, and $H = H_{\min} + i \cdot \triangle H$.

Since Equation (10) shows that H has a direct relation with consequences, the relationship in Equation (16), presented in Figure 4 as well, is the equivalent of the F_D-curve and F_N-curve as used in Jonkman et al. (2016) and schematic given in Figure 2(C). We will refer to these curves as F_H-curves. The integral of the surface below this figure is directly related to the risk in Equation (4). Multiplied by the polder surface A and damage coefficient c_d, it is calculated by the discretization in Equation (18).

3.4 | Probabilistic approach

Even with the simplifications as presented in the sections before, the calculation of Equation (18) is time-consuming. Furthermore, because of the discontinuity of $\hat{h}_{\vec{X}}$, due to a possible dike breach during an event, a FORM technique is not applicable without significant additional measures for numerical stability. Therefore, the probabilities of exceedances are assessed by a Monte Carlo importance sampling (MC-IS) method. The benefit of an MC approach is the independence of calculation time from the number of stochastic variables. Implementation of this approach requires some additional starting points:

- Package: The free available software package Probabilistic ToolKit (Brinkman, 2021) developed by Deltares is used. This package calculates probabilities for a given limit state function for a variety of probabilistic techniques including MC-IS.
- Importance sampling: The choosing of the important $\vec{X}$-space around a central IS-point is subjective and for each value of H, this may shift a bit. Therefore, an iterative procedure has been used that is developed in PTK, in which in several loops, the IS-point is adjusted to get a sufficient accurate result. This is done for each individual calculation in a series of calculations.
- Time base: The duration of the load event on the system is taken as long as the longest load event involved, $T_{\max}$. For a riverine area that is the period of a river flood wave, for the Rhine in the Netherlands about 1 month (Chbab, 2016). These periods are considered to be independent. Upscaling of probabilities to a year, the time unit mostly used for

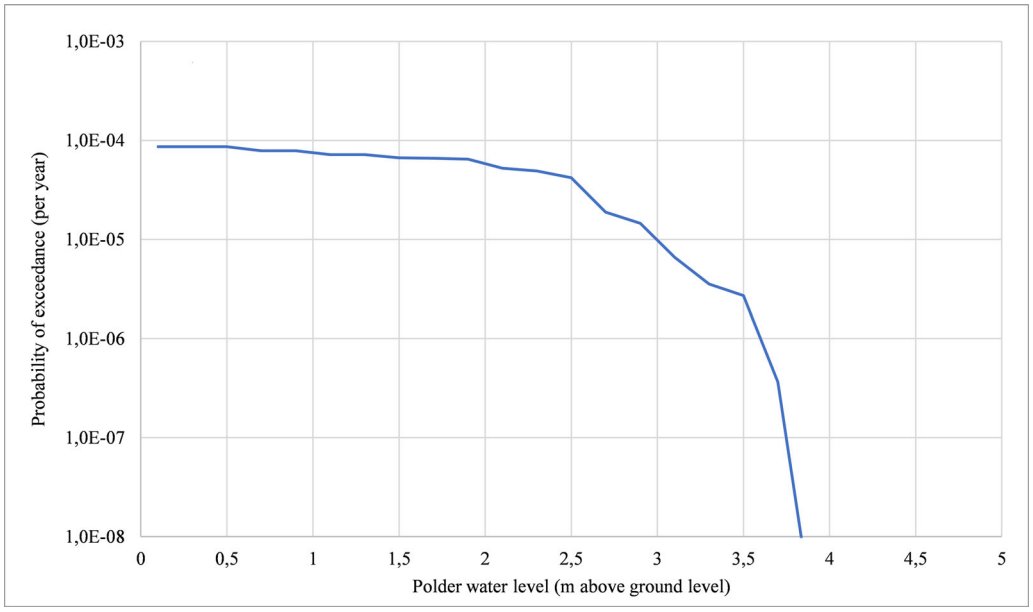

FIGURE 4 Example of a series of probabilities of exceedance of polder water level *H*.

flood risk analyses is a simple analytical transformation of Equation (16):

$$\forall H \in (0, dike\ crest) : P_{yr}(\hat{h}_{\vec{X}} > H) = 1 - (1 - P_{T_{\max}}(\hat{h}_{\vec{X}} > H))^{\frac{T_{year}}{T_{\max}}} \tag{19}$$

- Combining loads with different time scales: During a river flood event, there may be several load events with a shorter time base. In this study, windstorms are included, causing waves that may damage the dike. These windstorms are modeled occurrence once at random in time within the flood event. This is an underestimation because there may be more windstorms during one event, but in a riverine situation, the discharge of the river flood wave is by far the most important stochastic variable, so this inaccuracy is expected to be very small.
- Wind direction: Each sample represents a flood event, composed based on the different load variables. The wind direction is one of them. For practical reasons, only one wind direction is chosen for the whole flood event.

Following this starting points, the load model has been compared with the load model HYDRA-NL as given by (Geerse et al., 2011) used for assessments and designs for the National Flood Protection Program in the Netherlands, for a location along the Rhine river, 906.300 km. The comparison is pretty good, see Figure 5 for both water levels and overtopping discharges.

In Figure 6, the calculation process for the MC-IS-analysis is schematized. For each drawn sample, the limit state function is evaluated, requiring a calculation of the physical model shown in Figure 3, resulting in $\hat{h}_{\vec{X}}$.

3.5 | Effect of climate change and subsidence

The effect of climate change is based on Smale (2018). The effect is represented in a transition of the probability distribution of the river discharge

$$Q = Q_{2015} \cdot \left(1 + c_{cl} \cdot (horizon - 2015)^{b}\right) \tag{20}$$

in which Q_{2015} represents the discharges base value in 2015, *horizon* is the year of interest, and c_{cl} and b depend on the climate scenario, see the Appendix.

Subsidence is assumed to occur equally for the whole cross section, leading to:

$$h_x = h_{x,2015} - \frac{dh_x}{dt} \cdot (horizon - 2015) \tag{21}$$

In which $h_{x,2015}$ represents the height in 2015 for location x in the dike cross section, and h_x the height for location x in the dike cross section in the year *horizon*. $\frac{dh_x}{dt}$ is the velocity of subsidence per year.

3.6 | Calculation of investments

The investments I to take measures in the cross section are based on initial investments, independent of degree and type of reinforcements, and the marginal investments due to supply, replace or removal of volume of materials used for the reinforcement, renewal of the pavement on the dike, or change of construction type such as the use of a sheetpile. In the Appendix, the full equation is given. The application of the marginal costs and parameters in this equation is based

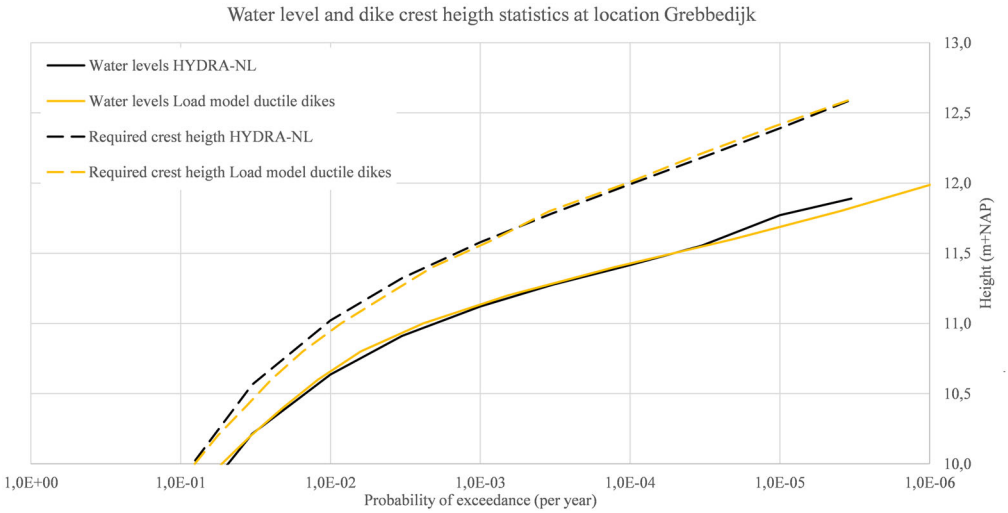

FIGURE 5 Comparison between the model HYDRA-NL (Geerse et al., 2011) (black lines) and the model in this article (orange lines) for water levels (solid lines) and required dike crest heights (dike heights corresponding with a required limit for overtopping discharges, in this case 1 l/m/s). Dike slope 1:3.

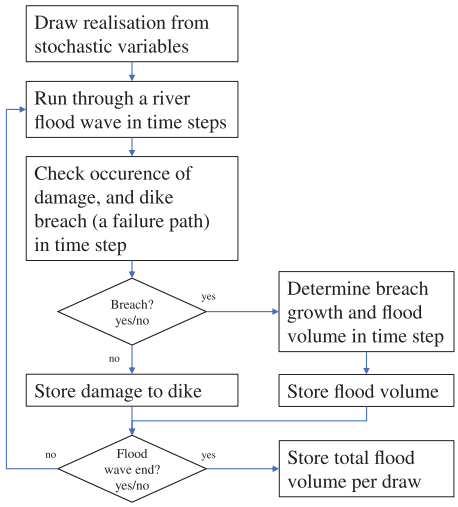

FIGURE 6 Flowchart of the evaluation of an individual limit state function.

on exercises with KOSWAT (de Grave & Baarse, 2011), the model used in the Dutch Flood Protection Program.

4 | APPLICATION IN CASE GREBBE

4.1 | Location

The location for the case is the "Grebbedijk," along the river Rhine branch "Nederrijn," at river 906.300 km, between dike marks 46 and 47, at the Paris coordinates (170757,140168), see Figure 7. For this case, location is chosen based on several criteria:

- the location has to be on primary dike in the Netherlands, along a large and independent source of risk (Kok et al., 2017);
- for a proof of concept of the methodology, a relatively simple load regime is preferred. Therefore, the riverine area has been chosen, with river flood waves as major load, without near-sea effects of high tides, and with wind speeds causing waves as secondary load;
- the dike has a risk deficit, urging the dike manager to reinforce.

4.2 | Case-specific starting points

To operationalize the concept for a riverine case, the following assumptions and starting points are made:

- Six dike construction types are considered, referring to Calle (2002), Breedeveld et al. (2019), and the DeltaCommision (2008) who recommended to consider Delta dikes: a traditional dike, a dike stabilized with a sheetpile, and a width dike, all with cores of sand or clay, see Figure 8. Types A and D are typical for the Dutch river area. These types are chosen because of the expected difference in ductility and corresponding risks.
- Two chosen design dimensions characterize the difference between the construction types in the calculations for this article: the top level of the sheetpile in construction types C and F is 1.5 m above the landward polder level, and the extra crest width of the construction types B and E with respect to the other types is 10 m.
- Loads and strengths are assumed to be homogeneous over the length of the dike segment of 5.5 km. Climate change and subsidence are deterministically coupled to the chosen design horizon in 2075, assuming climate scenario G+

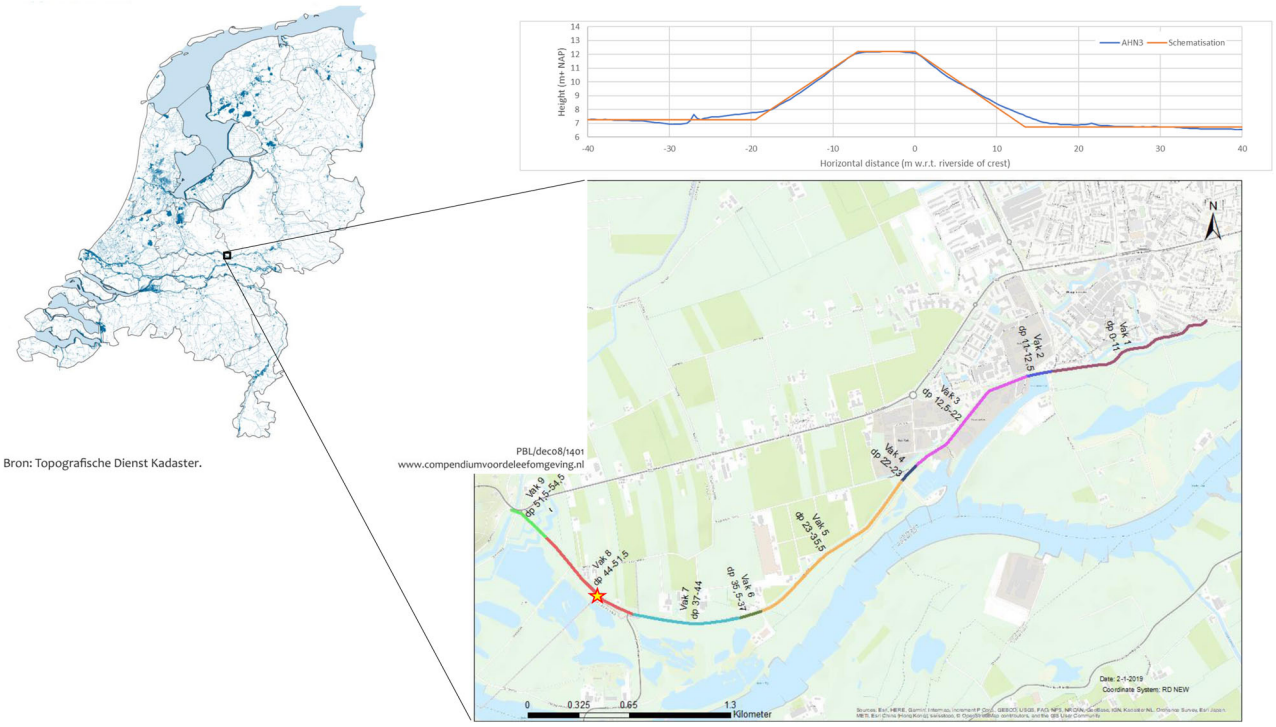

FIGURE 7 Map of the Netherlands (left) and the location with dike segment, dike section, and dike cross section of interest (right below). Profile of dike cross section: the national digital terrain model AHN3 in blue and the schematization for this study in orange (right above)

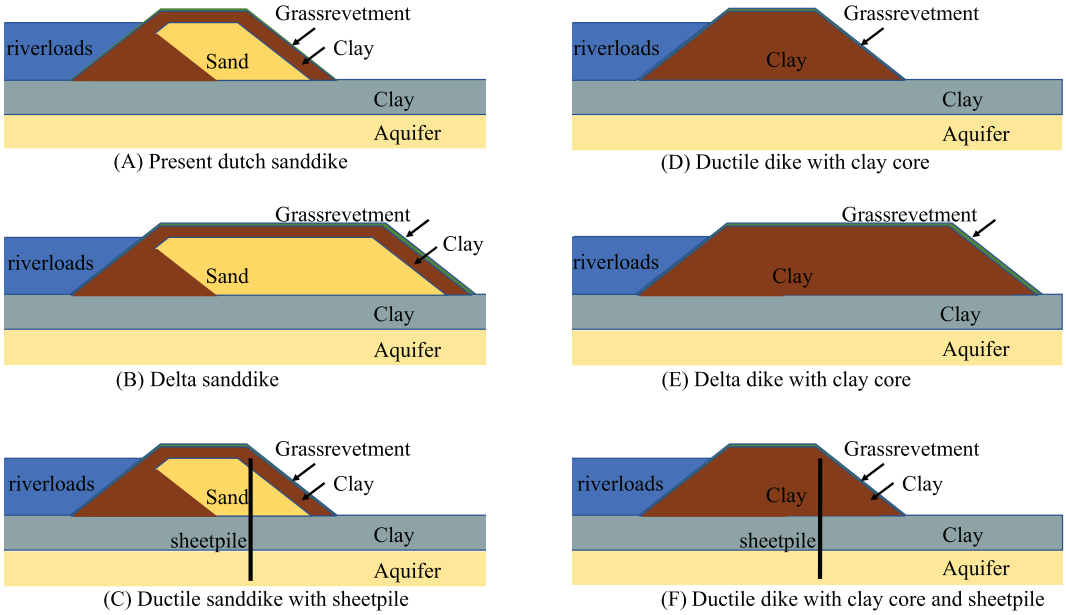

FIGURE 8 Six dike cross sections used for this study, typical to express the effect of ductile behavior on flood risk.

(Smale, 2018) and subsidence of 0.17 m/50 year (Hop, 2019).

- The probability distribution of the water level on the location of interest is based on the distribution of discharge in the Rhine river, which is based on the statistics at Lobith, available from load events (Chbab, 2016). Floodings upstreams are assumed to prevent flood waves exceedance of discharges 18,000 m^3 (MinVenW & ENW, 2007).

TABLE 1 Results of assessment for 2015 for existing dike at case location, with polder level 7.25 m+NAP. Second line in the rows represents the costs and risks in 2075 without measures with respect to the present situation.

Construction type (see Figure 8)	Dike height (m+NAP)	Berm width (m)	Berm height w.r.t. polder (m)	Soc. costs (total/I/ER) (M€ ,NPV)	Indiv.risk (vict./ha) ($\cdot 10^{-5}$/yr)	prob. dike failure ($\cdot 10^{-5}$/yr)
Existing	12.20	0	0	30.3 / 0 / 30.3	0.12	5.8
(d)				306 / 0 / 306	1.18	53.7
Semi-existing	12.20	0	0	47.8 / 0 / 47.8	0.18	6.8
(a)				393 / 0 /393	1.51	54.2

- The Rhine branch "Nederrijn" discharges 21%, independent of the exact discharge (MinVenW & ENW, 2007). Analytical relations are used between the national borders and the location of interest, derived based on a series of numerical calculations with SOBEK (Agtersloot et al., 2019).
- A flood wave on the Rhine river has a duration $T_{\max}$ of about 1 month, 675 h (Chbab, 2016). The probability in summer is assumed to be zero; thus, with T_{year} is 6*30*24 = 4320 h, about six independent flood wave events occur per year. The time step in the calculation of each MC sample is chosen as 1 h, small with respect to the event duration.
- Interest rate is assumed to be 3% and the value of a human live is based on Kind (2014) 6.7 M€ .

4.3 | Calculations, results, and analysis

The risks for the present situation (year 2015) have been assessed with the physical relations of Equation (3). The results are presented in Table 1. Note that the Societal Costs are in this case only the costs due to the risk of flooding. Two variants of the existing situation are presented: the existing dike with a clay core and a semiexisting situation, representing the same dike with a sand core. For both variants, no investment costs I are needed to reach the existing situation. Table 1 presents as well the situation in 2075 when no measures are taken, 10-folding the NPV and the number of victims. Note that the individual risks are expressed as the number of victims per hectare. This deviates from the LIR as presented in the decision framework, because an LIR could not be derived from this proof of concept schematization (hypothetical flat polder, 0-D hydraulic model) for which no postal code areas are available.

When measures are considered to reduce the risks, investments have to be made. Usually, optimizations of dike design as presented in Jonkman et al. (2016), Kind (2014), and den Heijer (2021) are used, searching for a dike failure probability resulting in minimal societal costs, or other criteria such as reduction of individual risks. For this optimization, mostly a limited number of design degrees of freedom are considered. In Kind (2014) and den Heijer (2021), the most important design variable is the dike height. The optimization searches for the dike failure probability resulting in the minimal societal cost. However, in this study, the dike failure probability or dike height is not sufficient information to assess the consequences of floods protected by dikes with different ductile behavior. The concept, summarized by Equation (18), even does not explicitly require the dike failure probability. Furthermore, for noneconomic criteria such as individual risks, this type of optimization does not hold, because no economic benefits exist for noneconomic criteria.

In this study, an optimization process had been set up, similar to Jonkman et al. (2016), Kind (2014), and den Heijer (2021), without the need of an explicit dike failure probability, and with the opportunity to compare the performance of different dike construction types. The heuristic optimization process for this approach is rather straight forward, but time-consuming:

- For the different dike construction types in Figure 8, different dimensions are taken. For the dimensions, a matrix of several combinations of dimensions has been taken, step by step enlarged with respect to the existing dimensions.
- For each construction-dimension-combination (in the following referred to as CDC), the exceedance curves of water levels F_H in the polder are calculated with Equation (16), and the corresponding risks are calculated with Equation (18).
- Each CDC corresponds to an investment as well. The investments I follow from the difference between the difference of the CDC with the existing situation.
- The costs and risks of all CDCs are graphical presented with the individual risks as the average number of victims per hectare per year on the x-axis and the societal costs on the y-axis.

The varied dimensions are crest height, berm width, berm height, and inner slope. Figure 9 gives examples for some F_H-curves for the different construction types in Figure 8. The shape of the F_H-curves is mainly a decreasing probability for increasing exceedance levels. They are more or less smooth. The slight angularity is caused by the limited number of MC samples, having minor effect on the risks. However, the curves for the sand core with sheetpile and to some extent the sand core with extra width show a sharp dip in the curves, caused by the interference of two different mechanisms piping and overtopping. Overtopping causes most likely dike breach, but due to the time needed to erode the crest, less

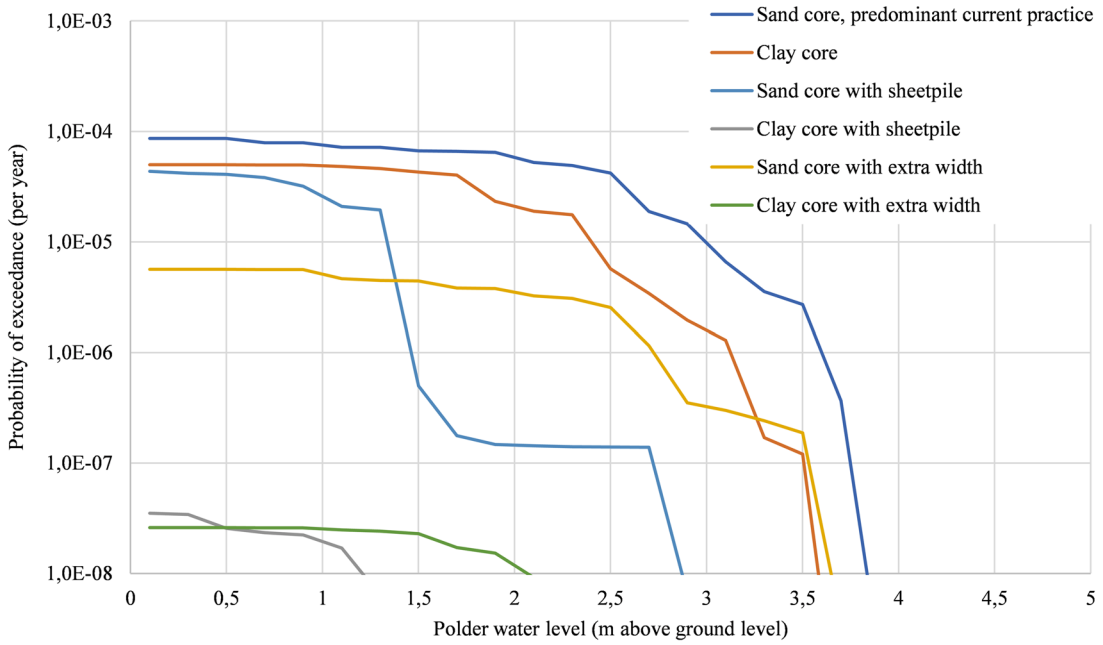

FIGURE 9 Examples of a series of probabilities of exceedance of polder water level H, for different construction types. Crest height = 12.2 m+NAP, Berm width = 10 m, Berm height = 0.75 m, and inner slope 1:2.5.

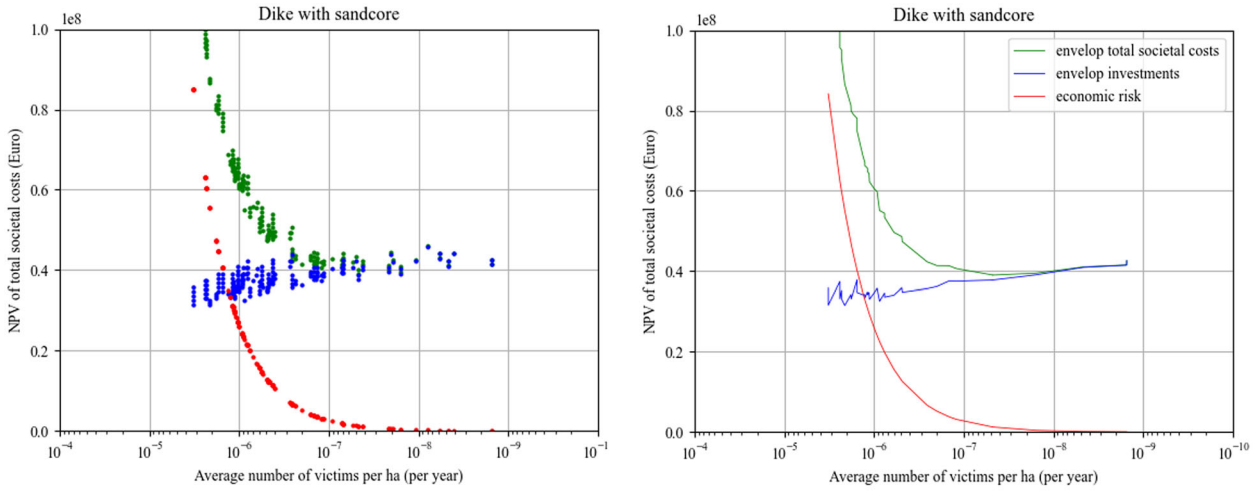

(A) Results for a matrix of dike dimensions, as input for heuristic optimization

(B) Bottom of envelop of societal costs, and corresponding investments and risk.

FIGURE 10 Societal costs related to corresponding individual risks

time is left to cause a large flood volume due to the sheetpile. Piping causes less likely a dike breach in this situation, but in case of a very large and long lasting river flood wave, it may cause breaches in a very early stage of the river flood wave, with more time to cause a large flood volume, even if the sheetpile reduces the breach discharge. The surface between the F_H-curves for the sand dike with sheetpile and the sand dike reflect the difference in risks, whereas the probability of dike failure is more or less equivalent. Thus, a sheetpile in the dike is a measure to increase the ductility, and thus, the structural robustness.

The results for numerous CDCs are calculated. In Figure 10(A), the results for different CDCs for construction-type "dike with sand core" are presented. A triple of dots represents one CDC, referring to, respectively, its economic cost, risk and investment on the y-axis, and its social risk on the x-axis. The dots representing the economic and societal risks do not scatter, because of their common source in the F_H-curve: following Equation (18), there is a fixed relation between them $c(d_{ER})/d_{nv}$. In Figure 10(B), the bottom of the envelop is shown of the total societal costs of all CDCs, together with the corresponding risks and investments.

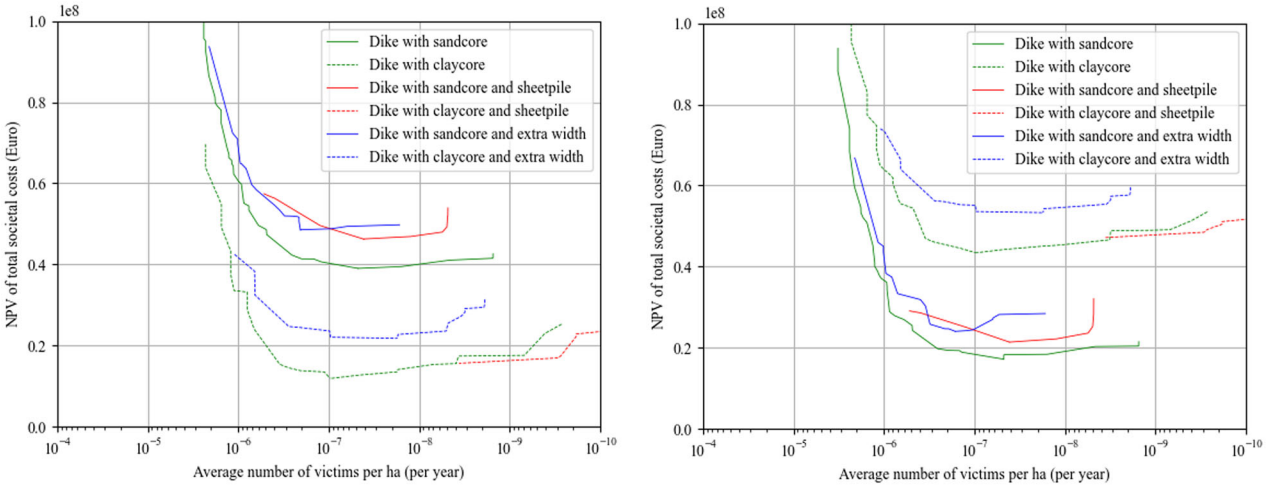

FIGURE 11 Envelops of societal costs for the different dike construction types from Figure 8

TABLE 2 Results of design calculations for existing clay dike at case location, with polder level 7.25 m+NAP. Inner slopes 1:2.5

Construction type (see Figure 8)	Dike height (m+NAP)	Berm width (m)	Berm height w.r.t. polder (m)	Soc. costs (total/I/ER) (M€ ,NPV)	Indiv.risk (vict./ha) ($\cdot 10^{-5}/yr$)	prob. dike failure ($\cdot 10^{-5}/yr$)
Sand core (a)	12.60	20	0.75	39.0 / 37.8 / 1.2	0.0048	0.17
Clay core (d)	12.20	20	0.75	11.9/ 9.4 / 2.5	0.0097	0.38
Sand core with sheetpile (c)	12.40	0	0	46.2 / 45.2 / 1.1	0.0041	0.41
Clay core with sheetpile (f)	12.20	0	0	15.6 / 15.5 / 0.1	0.0004	0.03
Sand core with extra width (b)	12.40	0*	0	48.5 / 43.2 / 5.3	0.0206	0.65
Clay core with extra width (e)	12.20	15	0.50	21.8 / 21.3 / 0.5	0.0017	0.07

*optimal inner slope 1:3.5.

It shows clearly the similarity with usual economic optimization practices. However, the x-axis does not contain a singular physical decision parameter. The neighbors of a CDC-dot with a certain position on the x-axis may be the result of a rather different combination of dike dimensions. Because of the discontinue multidimensional matrix of calculations, the envelop does not look that fluently in the high societal risk zone. However, the low societal risk zone is in this case more important for the determination of the optimum.

Figure 11 shows only the envelop of the total societal cost for all construction types. The left Figure 11(A) shows the results for design options with the existing clay dike as a starting point. The cost-optimal measure is the CDC with minimal societal costs. These are given in Table 2 for each construction type. For some of the curves, the optimum is the left edge of the curve. Just the change from the existing construction type to, for example, a dike with extra crest width will lead to minimal costs for that construction type. Enlarging one of the dike dimensions will increase societal costs. For some curves, the edges are shaped vertical, such as the right end of the curve for the dike with sheetpile. This is caused by the limited size of the matrix with dimensions calculated.

The right Figure 11(B) shows the results for design options with a semiexisting dike with a sand core as a starting point. The cost-optimal measures are given in Table 3 for each construction type. In this case, the option for widening the crest becomes more competitive as well. In all cases, a change of core material is far too expensive.

The existing dike at the case location is a dike with a clay core, which is in this case the type resulting in the lowest net present value. However, the reduction of the individual risk on victims may be a reason to change construction type, regardless of the extra costs. In this case, the construction type with a sheetpile (in dotted-red) diminishes the individual risk, requiring only a rather small budget extra.

5 | DISCUSSION

The objective of this article is to enable the evaluation and comparison of the risk reduction potential of dike construc-

TABLE 3 Results of design calculations for semi-existing sand dike at case location, with polder level 7.25 m+NAP. Inner slopes 1:2.5.

Construction type (see Figure 8)	Dike height (m+NAP)	Berm width (m)	Berm height w.r.t. polder (m)	Soc. costs (total/I/ER) (M€ ,NPV)	Indiv.risk (vict./ha) ($\cdot 10^{-5}/yr$)	prob. dike failure ($\cdot 10^{-5}/yr$)
Sand core (a)	12.60	20	0.75	17.2/16.0/1.2	0.0048	0.17
Clay core (d)	12.20	20	0.75	43.4/40.9/2.5	0.0097	0.38
Sand core with sheetpile (c)	12.40	0	0	21.4/20.3/1.1	0.0041	0.41
Clay core with sheetpile (f)	12.20	0	0	47.2/47.1/0.1	0.0004	0.03
Sand core with extra width (b)	12.20	10 [a]	0.50	24.1/19.8/4.2	0.0163	0.61
Clay core with extra width (e)	12.20	15	0.50	53.3/52.9/0.5	0.0017	0.07

[a] Optimal inner slope 1:3.

tion types, as a fourth measure next to lower loads, increase dike dimensions, and reduce vulnerability behind the dike.

This study demonstrates the possibility to perform an analysis providing insight in the relation between dike construction types, dike dimensions, societal costs, and societal risks. To value different construction types with respect to their effect on consequences of flooding, the whole chain from loads, strength, dike breach, flooding, and consequences is modeled time-dependent. The widely used practical cut between calculations of dike failure and consequences (Bischiniotis et al., 2018; VNK2, 2011) is not needed in this concept. The decision framework presented in Section 2.2 is generally applicable. We will discuss some benefits of this approach, the limitations of this study, and some recommendations.

First, this integral modeling enables the use of the risk concept in Jonkman et al. (2016) and Kaplan and Garrick (1981) in a basic way, using the number of MC samples as the flooding scenarios, which are directly used to take into account uncertainties in loads, strength, and consequences. Although failure of the dike is of major impact on a flooding, the physical processes are treated in the same way as other physical processes such as hydraulic modeling of the river, it has no preferred position in the setup of the risk calculation. This reduces the introduction of assumptions to assess the time-dependent boundary conditions for flooding scenarios. In the approach used in this article, the mechanisms determining dike stability (in most literature referred to as failure mechanisms) develop parallel to each other. This implies that no compilation is needed of failure probabilities per failure mechanism, which are correlated due to correlated hydraulic boundary conditions and dike material.

Second, an effect of the practical cut between dike failure and consequences is standardization of dike failure probabilities, as formalized in, for example, the Netherlands. However, not formal, standards in terms of probabilities related to dike failure are common practice in many flood risk studies in Deltas worldwide, using them as a starting point for dike design. The objective of a designer is to deliver a most efficient design compliant with these standards. Due to the practical simplifications and suboptimalization, this will not per definition comply to the most efficient risk reduction. Due to the practical cut between probability of dike failure and consequences, a brittle dike is often valued just as good as a ductile dike. This study shows an approach on how to value dikes on its risk reduction capacity, due to its degree of ductility, leading to more opportunities for structural robust design interventions.

Third, each model requires simplifications of reality, such as to cut parts of the physical processes, to simplify modeling of physical relations, to make choices to simplify the process in time, or to calculate probabilities. However, the approach in this study does not require simplifications due to the approach itself. The simplifications in this proof of concept can be extended, having only effect on calculation time. The approach in this study aims to hand over opportunities to choose simplifications based on their effect on dike dimensions, combined with practical applicability and accuracy.

A limitation is the application on only one case location situated in a riverine area, using a limited number of dike failure mechanisms. Consequently, we used only one dike breach location. In theory, along a dike segment, more breaches could occur. Although this is unlikely due to the water-level effect as a result of breaching (see Figure 3 upper part) that decreases the loads downstream of a breach, the concept can be extended to a series of dike locations. Equation (14) then has to be evaluated for all dike sections in a dike segment, and in $\vec{X}$, the independent variables per location should be added.

A second limitation is the 0-D representation of the flood simulation and the analytical coupled consequences in (10). Especially when we would expand the dike section to a gradually descending dike segment enabling more breaches along the river, this representation should be changed in the real bathymetry of the polder and a flood simulation model should be used.

However, not a conceptual limitation, only the flood waves during winter periods are taken into account in this article. The extreme discharges along the Meuse river in July 2021 showed that this starting point needs to be reevaluated.

The recommendations are mainly enhancements to elaborate and mature the application of the presented approach.

- For applications in other than riverine areas, the load regimes should include areas such as the deltaic, sea, and lake environments. For the riverine area, an iterative

analytical approach was implemented to present the effect of a breach on the near-breach river water levels. For other load regimes, and a riverine area near bifurcation points as well, a numerical hydraulic model is required to reflect the effect of a breach, which has a direct relation to the flood volume and thus to the risks of flooding in Equation (18).

- The dike failure mechanisms should be extended with other dike stability mechanisms. For example, the macrostability mechanism can be implemented when the time-dependent phreatic surface in the dike is modeled, as well as the remaining profile after different sliding surfaces. Furthermore, the physics of failure paths should be enhanced. For example, the erosion of a damaged dike profile is modeled by the NRCS derived from spillway research (NRCS, 1997).
- The consequences of a breach should be modeled for areas in which the 0-D approach is not accurate. In this area, implementation of a proxy, or a full numerical model should be possible, as well as implementation of models for calculating 2D consequences in an area.
- Above-mentioned recommendations require extra calculation time. Two improvements should be considered in the existing approach. First, the presented optimalization heuristic method: simply calculating a matrix with as much ribs as degrees of freedom in the design is too time-consuming in cases with large matrices, as is the case for a dike segment with different reinforcement solutions for different dike sections. In such cases, solutions have to be implemented as a greedy search algorithm such as used in Klerk et al. (2021). Second, the use of calculation clusters with multiple cores. However, not that complex, this will enlarge the attractivity to use the benefits of this approach.

6 | CONCLUSIONS

In this article, we present a novel assessment method for evaluating the risk reduction potential of dike construction types. Next, to reduction of loads, increase of strength, both reducing the probability of failure, and reduction of consequences of dike failure, this opens the route for a fourth category of risk reduction measures: structural robust dike design. We showed that the risk profile of different construction types may differ significantly. We also presented a method and graphical representation to compare designs based different construction types.

Several novel elements are included in the approach. Most importantly is we do not need to explicitly calculate the dike failure probability, because the risk is defined as the probability of a certain flood level at a location in the polder times the consequences of that flood level. The whole process of loads by the water system, strength- and erosion development of the dike, breaching, and flooding are integrated modeled time-dependent in the physical domain. This provides a novel insight of the simultaneously propagation of the development of the failure mechanisms in time, including possible interactions. In the Grebbe case, this approach led to significantly different risk profiles in case the polder is protected by a brittle or a ductile dike.

The main conclusion of this article is that an integrated risk assessment, based on a time-dependent physical model, provides the insight in the difference in risks between brittle and ductile dikes, enabling the trade-offs of dike designs and corresponding risks and investments.

Due to the integrated approach, a suboptimal application of the risk approach can be prevented. Furthermore, several techniques or practices are no longer needed, reducing the number of design choices. For example, techniques used to explicitly calculate or assess the dike failure probability, such as a fault tree analysis to combine different dike failure mechanisms, or to explicitly choose representative flooding scenarios to calculate the risk.

The implementation of the approach shows a simple understandable result: a set of dike constructions and dike dimensions leads to corresponding flood-level probability curves, which are the base for the corresponding economic and individual risk. The presented graphical connection between the societal costs and the individual risks provides a powerful insight to enable trade-offs between construction types.

The method is implemented for a riverine water system. For the implementation in a proof of concept, some simplifications are made to be able to perform a case study to show the analysis and results of the method. The main simplifications, such as the implementation of only two dike failure mechanisms, and the use of a 0-D flood model, are easily extendible. However, enhancements of optimization routines and calculation power need to be considered.

Our interpretation of the conclusion is that evaluation of structural robustness should be standard in dike design. This would further mature the flood risk approach, leading to well-considered designs, with a ductility dependent on the potential consequences. Fully implemented, with ductile dikes at high-risk locations, the consequences could be mainly economic damage, which would simplify the trade-offs. Therefore, we recommend further steps to develop the method for other than riverine systems, and to operationalize the method for application in Flood Protection Programs.

ACKNOWLEDGMENTS

The authors would like to thank the editors and anonymous reviewers for their insightful comments that significantly improved the manuscript. The authors would like to thank the efforts of R. Brinkman from Deltares, for his extensions of the probabilistic toolkit enabling the calculations for this article, and HAN University of Applied Sciences for their support to enable this publication. We disclose any funding or other competing interests.

REFERENCES

Agtersloot, R., van der Veen, R., & van der Veen, S. R. (2019). *Betrekkingslijnen Rijntakken, versie 2018*. Technical report, 4500283440, RURA-Arnhem.

Baker, J. W., Schubert, M., & Faber, M. H. (2008). On the assessment of robustness. *Structural Safety*, *30*(3), 253–267.

Bischiniotis, K., Kanning, W., Jonkman, S., & Kok, M. (2018). Cost-optimal design of river dikes using probabilistic methods. *Flood Risk Management*, *11*, S1002–S1014.

Breedeveld, J., Zwanenburg, Z., Van, M., & Lengkeek, H. (2019). Impact of the Eemdijk full-scale test programme. In *Proceedings of the XVII European Conference on Soil Mechanics and Geotechnical Engineering ECSMGE-2019*. International Society for Soil Mechanics and Geotechnical Engineering.

Brinkman, R. (2021). Probabilistic Toolkit.

Calle, E. (2002). *Dijkdoorbraakprocessen*. Technical report, 720201/39, GeoDelft.

Chbab, E. (2016). *Waterstandsverlopen Rijntakken en Maas*. Technical report, 1220082-002-HYE-0002, Deltares.

de Bruijn, K., & Klijn, F. (2011). *Deltadijken: locaties waar deze het meest effectief slachtofferrisico's reduceren*. Technical report, 1202628-000-VEB-0005, Deltares.

de Bruijn, K., & van der Doef, M. (2011). *Gevolgen van overstromingen - Informatie ten behoeve van het project Waterveiligheid in de 21e eeuw*. Technical report, 1204144-004-ZWS-0001, Deltares.

de Grave, P., & Baarse, G. (2011). *Kosten van maatregelen, informatie ten behoeve van het project Waterveiligheid 21e eeuw*. Technical report, 1204144-003-ZWS-001, Deltares.

DeltaCommision (2008). *Samen werken met water Een land dat leeft, bouwt aan zijn toekomst Bevindingen van de Deltacommissie 2008*. Technical report.

den Heijer, F. (2021). Adaptive flood defence management with ductile dikes. In A. Chen, X. Ruan, & D. Frangopol (Eds.), *Proceedings of the 7th International Symposium on Life-Cycle Civil Engineering (IALCCE 2020)* (pp. 471–478), Shanghai, China. CRC Press.

Eijgenraam, C. J. J. (2006). *Optimal safety standards for dike-ring areas*. Technical report, ISBN 90-5833-267-5, CPB Netherlands Bureau for Economic Policy Analysis.

Geerse, C., Slomp, R., & de Waal, H. (2011). *Hydra-Zoet Probabilistic model for the assessment of dike heights: Probabilistic model for the assessment of dike heights*. Technical report, PR2168, HKV consultants, Ministry of Infrastructure and Environment, Deltares.

Halter, W., Groenouwe, I., & Tonneijck, M. (2018). *Handboek Dijkenbouw, Uitvoering, versterking en nieuwbouw*. Hoogwaterbeschermingsprogramma, HWBP.

Helpdesk Water (2020). National database flood simulations.

Hop, M. (2019). *Technisch ontwerp zeef 2 verkenning Grebbedijk*. Technical report, 17M3041-R-015-V02, Lievense CSO Infra B.V.

Jonkman, S., Steenbergen, R. D., Morales-Nápoles, O., Vrouwenvelder, A., & Vrijling, J. (2016). Probabilistic design: Risk and reliability analysis in civil engineering. In *Collegedictaat CIE4130*.

Kaplan, S., & Garrick, B. J. (1981). On the quantitative definition of risk. *Risk Analysis*, *1*(1), 11–27.

Kind, J. (2014). Economically efficient flood protection standards for the Netherlands. *Journal of Flood Risk Management*, *7*(2), 103–117.

Klerk, W. (2022). *Decisions on life-cycle reliability of flood defence systems. Delft University of Technology*. (Draft), Delft University of Technology.

Klerk, W., Kanning, W., Kok, M., & Wolfert, R. (2021). Optimal planning of flood defence system reinforcements using a greedy search algorithm. *Reliability Engineering and System Safety*, *207*, 107344.

Knoeff, J., & Ellen, G. (2012). *Verkenning deltadijken*. Technical report, 1205259-000-ZWS-0004, Deltares.

Kok, M., Jongejan, R., Nieuwjaar, M., & Tanczos, I. (2017). *Fundamentals of flood protection*. ISBN 978-90-8902-160-1. Ministry of Infrastructure and the Environment & Expertise Network for Flood Protection.

Kortenhaus, A., & Oumeraci, H. (2009). Flood risk analysis and management in Europe - The way ahead. In *ICCE2008* (pp. 4214–4226). World Scientific Pub Co Pte Lt.

Mens, M. J. P. (2015). *System robustness analysis in support of flood and drought risk management*. PhD thesis, TU Delft.

Ministerie van Infrastructuur en Milieu (2016). Wet van 2 november 2016 tot wijziging van de Waterwet en enkele andere wetten (Waterwet).

MinVenW & ENW (2007). *Technisch Rapport Ontwerpbelastingen voor het rivierengebied*. ISBN 978-90-369-1409-3, Ministerie van Verkeer en Waterstaat & Expertise Netwerk Waterkeren.

NRCS. (1997). Field procedures guide for the headcut erodibility index. In *National engineering handbook, Part 628 Dams*, chapter 52. Natural Resources Conservation Service.

Rosenbrand, E., & Knoeff, J. (2020). *KvK 2019 onderzoek faalpaden en piping*. Technical report, 11203719-028-GEO-0009, Deltares.

Sayers, P., Hall, J., & Meadowcroft, I. (2002). Towards risk-based flood hazard management in the UK. *Proceedings of the Institution of Civil Engineers - Civil Engineering*, *150*(5), 36–42.

Slager, K. (2003). *De ramp, een reconstructie van de watersnood in 1953*. ISBN 9789045008158, Atlas.

Slomp, R., Knoeff, J., Bizzarri, A., Bottema, M., & de Vries, W. (2016). Probabilistic flood defence assessment tools. *E3S Web of Conferences*, *7*, 03015.

Smale, A. J. (2018). *Werkwijzer bepaling Hydraulische Ontwerprandvoorwaarden, Aanvulling OI2014, versie 5 (Hydra-NL 2.4.1)*. Technical report, 11202226-009-GEO-0002, Deltares.

Steenbergen, H., Lassing, B., Vrouwenvelder, A., & Waarts, P. H. (2004). Reliability analysis of flood defence systems. *Heron*, *49*(1), 51–73.

Steenbergen, H., & Vrouwenvelder, A. (1999). *Theoriehandleiding PC-RING versie 4.0, Deel C: Rekentechnieken*. Technical report, 98-CON-R1204, TNO.

te Nijenhuis, A., Hüsken, L., Diermanse, F., van der Meer, A., Jongejan, R., & Pol, J. (2020). *Faalpaden - Conceptuele analyse van het gebruik van de faalpaden-methodiek voor het bepalen van overstromingskansen in Nederland*. Technical report, 11203719-024-GEO-0016, Deltares.

van Dantzig, D. (1956). Economic decision problems for flood prevention. *Econometrica*, *24*(3), 276.

van de Ven, G. (2004). *Man-made lowlands: History of water management and land reclamation in the Netherlands*. Utrecht: ISBN 978-90-5345-191-5, Matrijs.

van den Ham, G. (2020). *Faalpadenanalyse macrostabiliteit binnenwaarts*. Technical report, 11203719-027-GEO-0001, Deltares.

van Hoven, A. (2014). *Residual dike strength after macroinstability*. Technical report, 1207811-013-HYE-0001-gbh, Deltares.

van Westen, C. (2005). *Veiligheid Nederland in Kaart. Hoofdrapport onderzoek overstromingsrisico's*. DWW-2005-081 ISBN 90-369-5604-8, Ministerie van Verkeer en Waterstaat - Rijkswaterstaat.

VNK2 (2011). *De methode van VNK2 nader verklaard - de technische achtergronden*. HB 1267988, Projectbureau VNK2.

Vrijling, J. K., van Hengel, W., & Houben, R. J. (1995). A framework for risk evaluation. *Journal of Hazardous Materials*, *43*(3), 245–261.

Vrijling, J. K., van Hengel, W., & Houben, R. J. (1998). Acceptable risk as a basis for design. *Reliability Engineering and System Safety*, *59*(1), 141–150.

SUPPORTING INFORMATION

Additional supporting information can be found online in the Supporting Information section at the end of this article.

How to cite this article: den Heijer, F., & Kok, M. (2022). Assessment of ductile dike behavior as a novel flood risk reduction measure. *Risk Analysis*, 1–16. https://doi.org/10.1111/risa.14071